Development of Disaster-Responding Special-Purpose Machinery: Results of Experiments

Jin Tak Kim[1], Sangshin Park[1], SangChul Han[1], Jinhyeon Kim[1], Hyogon Kim[2], Young-Ho Choi[2], Jaehong Seo[1,3], Sanguk Chon[1,4], Jungyeong Kim[1,4], and Jungsan Cho[1]

[1]Applied Robot R&D Department, Research Institute of Convergence Technology, Korea Institute of Industrial Technology
[2]Intelligent Robotics R&D Division, Korea Institute of Robotics and Technology Convergence
[3]Intelligent Robot Engineering, University of Science & Technology
[4]Robotics and Virtual Engineering, University of Science & Technology

October 21, 2021

Abstract

The frequent occurrence of disasters has prompted the development of efficient disaster-responding equipment. This study deals with the design of special-purpose machinery and its performance assessment. We defined scenarios through the environmental analysis of disaster situations and expert consulting. We also formulated a set of design specifications by analyzing the objectives of the tasks that must be performed at disaster sites, based on simulated scenarios and existing disaster response machinery. The disaster-responding special-purpose machinery was designed to perform various tasks and display rapid movement in disaster situations. And this paper presents the control structure configured to operate the developed machinery. The performance of the special-purpose machinery was assessed through different scenario tests.

1. INTRODUCTION

Large disasters have frequently been occurring across the world due to urbanization and climate change. Rapid response within the golden hour is essential to minimize the loss of lives and secondary damage at the disaster sites. Firefighters generally enter the site and perform rescue operations because secondary damage factors exist in these areas due to additional collapse and leakages. Robotic technologies are applying to increase efficiency while reducing the problematic conditions and risks faced by firefighters. Many research institutes are developing various technologies for use in actual disaster situations (Delmerico et al., 2019).

It is difficult for firefighters or robots to enter into a collapse due to large debris, delaying the rescue. Large debris is dismantled or moved to secure the access roads and support the rescue operations of the firefighters. Excavators, widely used, are usually optimized for digging, making it difficult to do other tasks in unstable environments after the disaster. In addition, there are vast differences in the workability of the excavators due to the varying skill level of the drivers. The excavator uses the excavator's arm to get on and off the truck, and the broken road also moves. Despite this ability to move to dangerous areas, it is not easy to move quickly because risks are scattered throughout the disaster. Using the operation method of the traditional excavator, the driver calculates the speed command of each actuator for the whole motion, which is not an easy task even for an experienced driver. As a result, the excavators take a long time to enter the site because they move by using the arm and the swing joint due to their limited mobility. The anxiety of failing in situations that may compromise the safety of the driver also limits rapid responses. Thus, there is a need for equipment capable of agile movement and fast precision work in unstable environments.

Many researchers are studying to improve efficiency and safety by applying robot technology, which has developed significantly during the last decades, to heavy machinery such as construction machinery. By utilizing the existing hardware components of the demolition machine BROKK 170 and the CAN bus protocol, there is a study to control the teleoperated machine from the cartesian coordinate control instead of individually controlling each axis with joysticks (Lee & Brell-Cokcan, 2021). For intuitive control of the operator, it is necessary to develop a master device for operating the machine. A study applies the haptic joystick feedback to remotely manipulate the excavator arm to help alleviate operator error in loading operations (S, Sairam, Veeramalla, Kumar, & Gupta, 2020). Since teleoperated excavators are more challenging to obtain information of the machine posture and the work object conditions than when boarded, there is a risk of overturning or falling when digging the ground. To solve this problem, providing feedback on the machine instability and an intuitive visual presentation to the operator is also being studied (Ito, Raima, Saiki, Yamazaki, & Kurita, 2021). However, it is not intuitive to control the machine with a joystick, so robot technology is required. Robotic technology can flexibly solve mobile manipulation tasks with a complex robot with dual-arm and a mobile platform through a telepresence suit and a user interface (Klamt et al., 2019). According to a recently published paper, there is content on a perceptual and identification pose planning system that autonomously manipulates large-scale irregular objects by gradually constructing a LiDAR-based map with an automated study of robot walking excavators. Based on this information, collision-free grasping poses for the robotic manipulator were planned to track these objects during manipulation while simultaneously picking and placing these objects. Instead of simply placing stones in user-predefined positions, complete 3D constructions of the grasped objects are generated and calculated just before placing the desired pose of each stone. ETH, Switzerland, showed the autonomous hydraulic excavator HEAP that made a drystone wall with irregularly shaped rocks (Mascaro, Wermelinger, Hutter, & Chli, 2020). Although many research institutes carry out various studies, it still seems necessary to develop machines suitable for disaster situations and technologies to operate them.

It is challenging to define tasks in the disaster situation, and the machinery must perform complex tasks under various conditions. There is a limit to the work that one can do with one arm. For example, cutting unfixed rebar with one arm is a difficult task. The machinery must have a different mechanism from conventional excavators to overcome obstacles and quickly access the disaster site. Therefore, the machinery for performing various functions in the disaster situation is being developed.

Various types of disaster response equipment are under development globally. The Korea Institute of Robotics and Technology (KIRO) developed an armored robot system that can be deployed in complex disaster sites (Jeong, Kim, Kim, Suh, & Jin, 2017)(Park et al., 2018). KIRO designed a car frame for the dual-arm manipulator to remove heavy obstacles, cut walls made of sandwich panels, and protect passengers from falling objects, toxic gas, and high temperature.

Hitachi's ASTACO (Ishii, 2006)(Machinery, 2012) is an example of the symmetrical implementation of two working machines on the body of an existing excavator and is called "an excavator with two fronts". The large model (NEO) is primarily used for dismantling buildings. The equipment deployed in the Tokyo Fire Department weighs 7 tons and has symmetrical fronts—each of which comprises 6 joints.

Tmsuk's T-52 comprises two arms, each of which consists of 6-DOF. Each arm has an attachment that can perform different functions and also provides an additional DOF. The operator can directly ride and manipulate the equipment; however, it also supports remote control to perform rescue operations in locations rescuers cannot access (Nishida et al., 2006).

The Guardian GT, manufactured by Sarcos (Salt Lake City, Utah, USA), is a dual-arm robot designed to efficiently transport heavy objects in an unstructured environment in industrial sites by modifying the system manufactured by Ditch Witch and attaching big arms (Sarcos Guardian® GT Robot, 2018). Beginners can easily manipulate the Guardian GT because it has a human-like structure and follows human movements.

KRAFT used a Brokk machine to design a manipulator with 6-DOF mounted on a mobile platform with two crawlers. It was designed for remote control operations at building demolition sites. 4-outriggers can be unfolded in the front, rear, left, and right directions to prevent the manipulator from overturning during work (Montazeri & Ekotuyo, 2016). Tadano's ROBOTOPS had a body with two arms and could walk on four legs and move using tracks (Robotops, 2009).

As shown in the examples discussed above, various disaster-responding systems have been developed across the globe. As shown in the example mentioned above, many research institutes worldwide are developing different disaster response systems. It remains a challenge to combine manipulation skills with the ability to perform on rough terrain. Many studies are designing dual-arm manipulators that can move quickly and simultaneously to overcome the limitations of existing excavators.

Figure 1: The disaster-responding special-purpose machinery.

We analyzed the environment for potential disasters and developed specific scenarios with the consultation of experts. Following that, the objectives of the tasks to be performed and the capabilities of existing disaster-responding systems are analyzed, and a set of design specifications are derived. Special-purpose disaster-responding machinery, based on the derived design specifications, was developed while ensuring that the system can perform various tasks efficiently and move rapidly at disaster sites, as shown in Fig.1. The machinery developed in this study comprises symmetrical manipulators with 7 DOF on the left and right, with a multifunctional, multi-branch attachment on each manipulator. The driving system has four legs with 2 DOF and an independently driven crawler at the end of each leg. The mainframe has a power pack and a swing joint. It consists of a single-person cabin and master devices to drive the system.

The system and the control methods need to be designed according to the movement and workability of the drivers. This allows the system to perform complex tasks with fast movement at a disaster site with crowded debris. Unlike conventional excavators that control one 4-DOF manipulator using two human arms, the disaster-responding special-purpose machinery proposed in the current study uses robotic technology to enable firefighters or other drivers to easily and intuitively manipulate the system. Thus, this study proposes developing a special-purpose machinery system and analyzes its performance in a simulated disaster environment.

This paper is organized as follows. Chapter 2 describes the scenarios derived through an analysis of disaster environments and the system specifications required to tackle these scenarios. The dual-arm manipulators, driving system, cabin, hydraulic system, and control network system are discussed in Chapter 3. Chapter 4 includes the control architecture designed to control the system. Chapter 5 describes the details of the experiments conducted in this study, and the concluding remarks are presented in Chapter 6.

2. DESIGN SPECIFICATIONS

In other to design the disaster-responding special-purpose machinery must define objective work and environment before deriving design specifications. We determine the test scenarios by consulting experts and analyzing the environment for disaster situations. The chosen scenarios were a series of events that could occur while rescuing people from the site of a building collapse–a common situation in disasters.

A building site is an uneven terrain with a pile of building debris inclined in different directions. Therefore, the driving scenario involved accessing the site after rapidly overcoming various terrains such as irregular road surfaces, slopes, and stepped obstacles.

The work scenarios involved lifting large debris, crushing cement debris, and cutting steel bars to secure an access road to transport equipment or firefighters to the site. The scenarios also include lifesaving actions like safely removing debris accumulated on buried people, spreading out structures such as doors or walls to secure an exit for trapped people, and pushing debris.

The required tasks and motions were classified according to the aforementioned driving and work scenarios. The objective specifications for each mission are defined in Table 1.

We derive the design specifications of the disaster-responding special-purpose machinery through defined task objectives and existing equipment analyses based on the following scenarios.

Table 1: Objectives of scenario tasks

Type	Task	Goal
Driving	Flat surface	4.1km/h
	Slope	Lateral side slope 15°
		Longitudinal slope 11°
	Uneven terrain	Driving on an irregular road surface with 10cm or smaller debris
	Overcoming steps	Passing through a 50cm high obstacle
Work	Lifting	400 kg at maximum reach
	Crushing	Crushing a concrete block
	Grabbing (Lifting)	Lifting a tire weighing 200 kg
	Pushing	Pushing drums
	Cutting	Cutting a 20mm thick steel bar
	Spreading	Tearing open a 0.5mm thick corrugated iron

- Maximum reach: The distance from the center of the main frame's swing bearing to the attachment mounted in the manipulators must be no shorter than 6m.
- DOF: The one-arm manipulator joint, attachment, and leg joints must have 7 DOF, 1 DOF, and 2 DOF, respectively.
- Lifting force: The system should be able to lift to 1 ton per arm. It should also lift 200 kg per arm, excluding the attachment's weight, at the maximum reach.
- Driving speed: The maximum driving speed of the complete system on a flat land must be 4.1km/h.
- Climbing ability: The maximum angle at which the complete system can climb while maintaining the position of the mainframe must be 30°

.

- Turning radius: The system must turn within a radius of 1.65 m from its center.

3. SYSTEM DESIGN

This section presents our platform's hardware setup and communication architecture, which is shown in Fig. 2. The following subsections discuss the design of each system according to the aforementioned design specifications and conditions. The core technologies for the major modules and indicate how they contribute to the satisfaction of the main system functions.

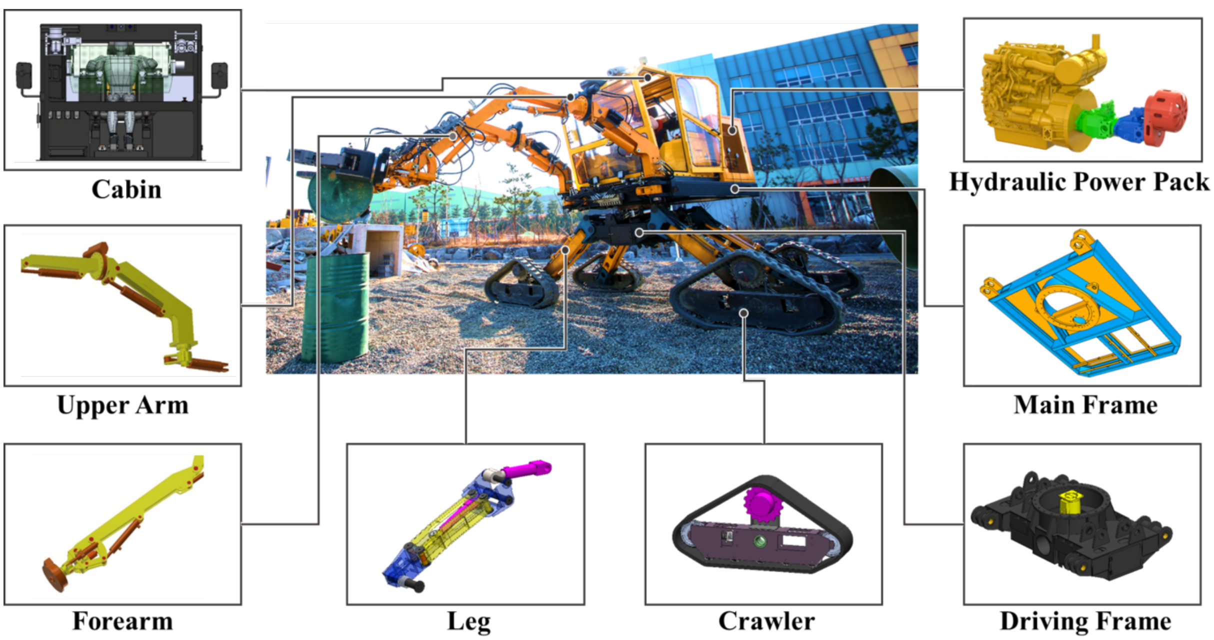

Figure 2: Overview of the disaster-responding special-purpose machinery.

3.1 Dual-Arm Hydraulic Manipulator

The manipulator shape must be designed according to the controllability of the system as it uses a combination of the driver's movements and robotic control technology. In addition to performing various tasks in an unstructured environment that meets the aforementioned design specifications, the manipulator system must perform two tasks simultaneously or individually and perform the same task in different ways. These include cutting a steel bar with one arm while grabbing it with the other or lifting an object that is difficult to grasp with one arm using both arms. Owing to their versatility mentioned above, many research institutes are extensively studying dual cancer systems.

The dual-arm manipulators to perform various tasks at the disaster site were designed by deriving design specifications to satisfy the developed scenario. In particular, the shape of the dual-arm manipulators was designed in consideration of the marionette control method to move well as intended by the operator so that firefighters can easily operate. Advantageously, the structure of the dual-arm manipulators is similar to the human arm to move accurately according to the human intention. The Robotics Research arms form a family of commercially available 7-DOF revolutes joint serial link manipulators that offer one extra degree of joint space redundancy over the primary task of end-effector placement and orientation. In brief, the dual-arm type manipulators can be kinematically represented by a 7-DOF configuration, i.e., a 3-DOF (Roll-Pitch-Yaw or Pitch-Roll-Yaw) shoulder portion, a 1-DOF (Pitch) elbow portion, a 3-DOF (Roll-Pitch-Yaw or Yaw-Pitch-Roll) wrist portion (Brantner & Khatib, 2020), (Klamt et al., 2019). The Yaw joint of the shoulder joint is essential for dual-arm cooperation, and the wrist joint of 3-DOF is required for the complex task and the dual-arm collaboration. Wrist designs capable of 3-DOF rotational motion can arbitrarily orient their end-effectors (up to a workspace limit). Wrists can improve manipulation capabilities, as they can orient the end-effector of a system without imparting significant translational motion. The role of the wrist becomes particularly significant when using a simple end-effector or when an object fully constrains the position of the end-effector, such as dual-arm cooperation.

The dual-arm manipulators were designed to ensure that the two arms can work together while conforming to the design specifications and conditions. When joints are set up by using hydraulic actuators, the range of motion (ROM) is relatively limited $90^\circ - 110^\circ$ in general. This joint structure arrangement affects the performance of the manipulators. To overcome this problem, the joint arrangement design was optimized by analyzing the work area of the dual-arm manipulators through the product of the total and common workspace area technique (PTCWA) proposed by Bagheri in a study that presented the specifications of the hydraulic actuator and the joint construction method (Bagheri, Ajoudani, Lee, Caldwell, & Tsagarakis, 2015). In this study, we design the joint structure of the manipulator according to the result carried out by the previous research (Cho et al., 2016), as shown in Fig. 3(a). $\{B_s\}$ is the reference coordinate of the dual-arm work manipulator. Joints $J_{A_1} - J_{A_4}$ were designed for translation motion, had a Yaw-Pitch-Roll-Pitch structure, and joints $J_{A_5} - J_{A_7}$ had a Pitch-Yaw-Roll structure to replicate the human wrist joint and its RoM. The ROM, piston diameter, and the joint torques of the designated joints are listed in Table 2.

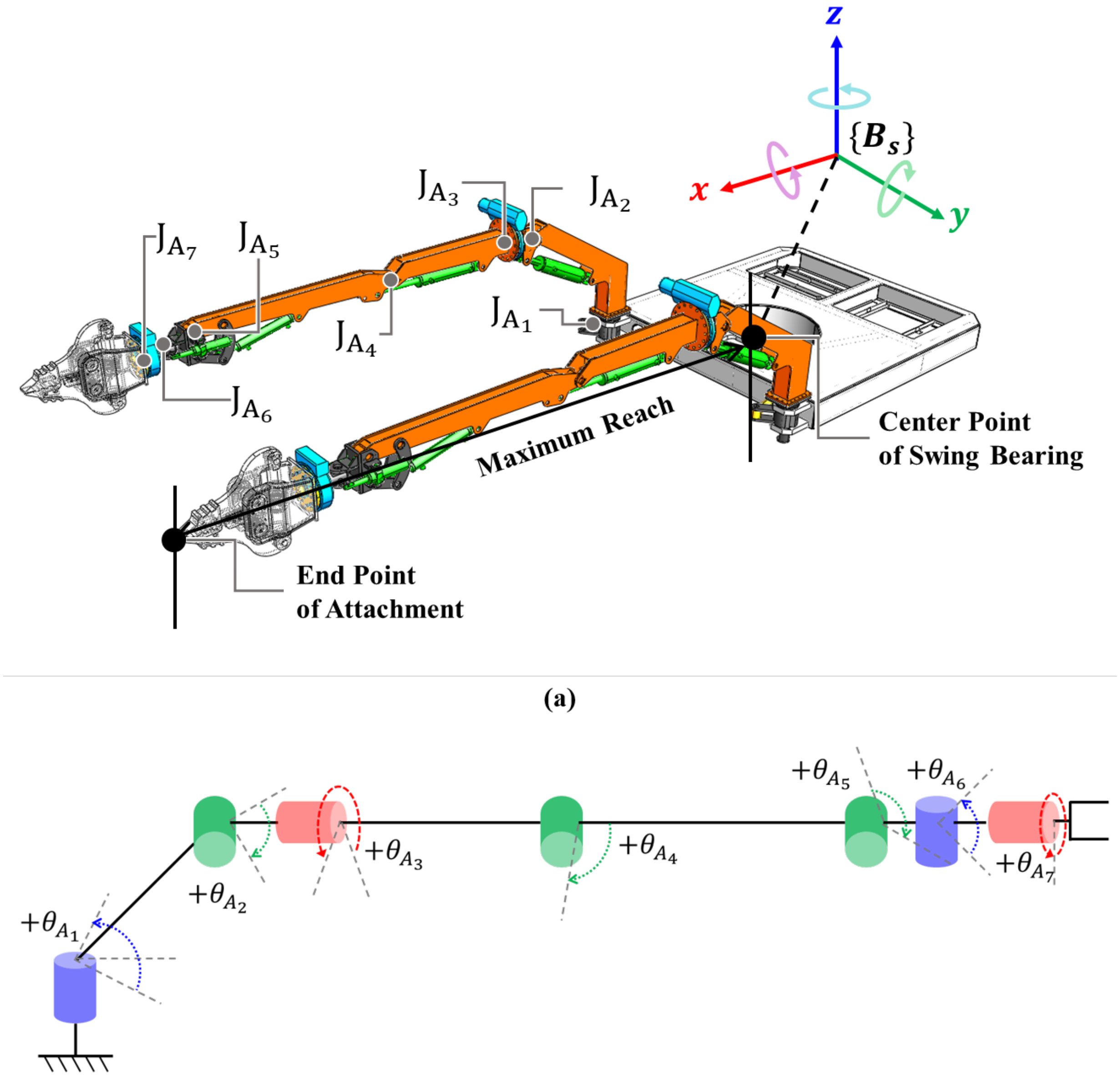

(b)

Figure 3: Structure of Dual-Arm Hydraulic Manipulator. (a) The manipulator features 7 actuated DOF. J_{A_i} represents the joint position, respectively. (b) Kinematic layout. Joint axes are marked with colored lines. Red, green, and blue represent roll, pitch, and yaw axes, respectively. θ_{A_i} is the angle of each joint.

A double-acting piston, a commonly used hydraulic cylinder in excavators, is used mainly in the joints of the dual-arm manipulator. The joint mechanism needs to be designed according to the working angle of the joint, and the actuator must account for the direction of gravity due to the difference between the tensile and compressive force. Figure 3(b) illustrates the kinematic scheme and joint positioning of the

Table 2: Specifications of Each Joint

Joint	Range of Motioin [°]	Diameter of the piston [mm]	Torque [kNm] at 140 bar	Axis
J_1	$-27 \leq \theta_1 \leq 63$	100.0	26.0	Yaw
J_2	$-30 \leq \theta_2 \leq 60$	90.0	22.7	Pitch
J_3	$-70 \leq \theta_3 \leq 70$	-	4.2	Roll
J_4	$0 \leq \theta_4 \leq 100$	70.0	11.7	Pitch
J_5	$-30 \leq \theta_5 \leq 110$	50.0	10.1	Pitch
J_6	$-45 \leq \theta_6 \leq 45$	50.0	4.0	Yaw
J_7	$-90 \leq \theta_7 \leq 90$	-	1.0	Roll

manipulator. The kinematics of the two arms closely resembles an anthropomorphic arrangement to provide a large workspace, to enable dexterous manipulation, and to simplify teleoperation.

We have manufactured the dual-arm manipulator, as shown in Fig. 4. It shows the location and structure of each joint manufactured and indicates the position of the valve manifold block. We confirmed the design specifications of the dual-arm manipulators in the previous study (Kim et al., 2020). The distance between the swing bearing center and the attachment connected to the manipulators is 6 m. The link connected to each joint was produced as a box-type welded structure. We checked the maximum lifting capacity through an experiment of hanging and lifting 1 ton of objects at joint 3. Also, we experimented with lifting 200 kg per arm, excluding the attachment's weight at the maximum reach. The position of the valve manifold block V_A #1 and V_A #2 was selected according to the positions of the driving joints and pipe connections as follows. In addition, we installed a hydraulic pipe to minimize interference and pressure loss during the functioning of the multiple joints.

Figure 4: eConfiguration of the dual-arm manipulator.

The cylinder in J_{A_1} is placed in the yaw axis according to the work performance of the dual-arm and the mechanical interference between them. The cylinder was mounted inside the mainframe to ensure that the end of the frame had a simple shape. This also created sufficient space to install 9-sections of Danfoss PVG valves (V_A #1), which are the control valves of the joints $J_{A_1} - J_{A_4}$ and the swing joint. The elements were designed to ensure the accurate movement of the entire manipulator while maintaining its stiffness. Joints J_{A_2}, J_{A_4}, and J_{A_5} are placed in the direction of the pitch axis. These joints are placed along the direction of gravity. The actuators used for these joints are designed according to the work performance and RoM requirements. For instance, J_{A_5} was designed to have a wide RoM of 140° by using a joint mechanism similar to that of the 4-bar structure, and its actuators were designed for lifting tasks. Joints J_{A_3} and J_{A_7} rotate in the roll direction by using a hydraulic motor and a worm gear. They were modified to have a wide RoM in a compact design space. Joint J_{A_6} rotates about the yaw axis by using two cylinders of the same size. Moog's G761 servo valve manifold (V_A #2) is attached to the forearm, which also serves as a control valve for joints $J_{A_5} - J_{A_7}$ and the attachment.

Every joint was mounted along with the non-contact sensor NRH300DP (Penny & Giles, Davidson, North Carolina, USA) to measure the rotational angle. A specific mounting device was designed for this purpose while accounting for the hydraulic hoses and adapters that supply hydraulic fluid to every cylinder.

A multifunctional attachment for performing a variety of tasks was attached to the right manipulator, while a gripper-type attachment for grabbing atypical objects was mounted at the end of the left manipulator. The attachments were designed by using the TRIZ method to respond to different tasks in situations of disaster (Cho, 2018).

In a disaster situation, we don't know what kind of work will be done. We need to have multiple attachment devices to deal with various tasks. In the case of excavators, attachments without actuators, such as buckets, have a removable mechanism that allows drivers to exchange only with skilled control. However, in the case of attachments with actuators such as breakers, share, and crushers, hydraulic lines must be connected by humans even if a mechanism connects it. The removable type can be exchanged for various tasks, while the exchange takes a long time, and the removable mechanism causes it to be large and heavy. Therefore, we design the attachment to respond to various tasks by separating the necessary functions without replacing the attachment, as shown in Fig. 5. In other words, the function that requires precise operation is on the right, the function of grabbing a variety of objects on the left, a large object can be held by both arms.

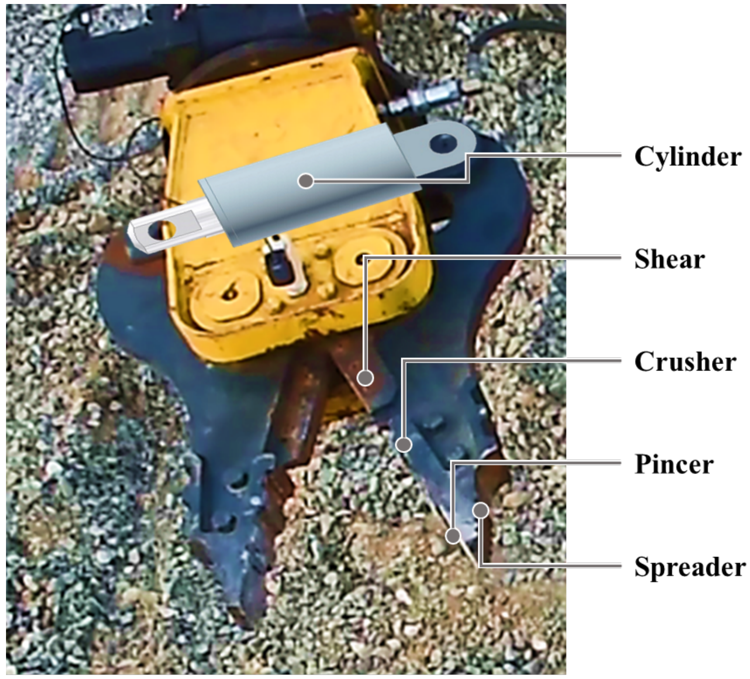

(a)

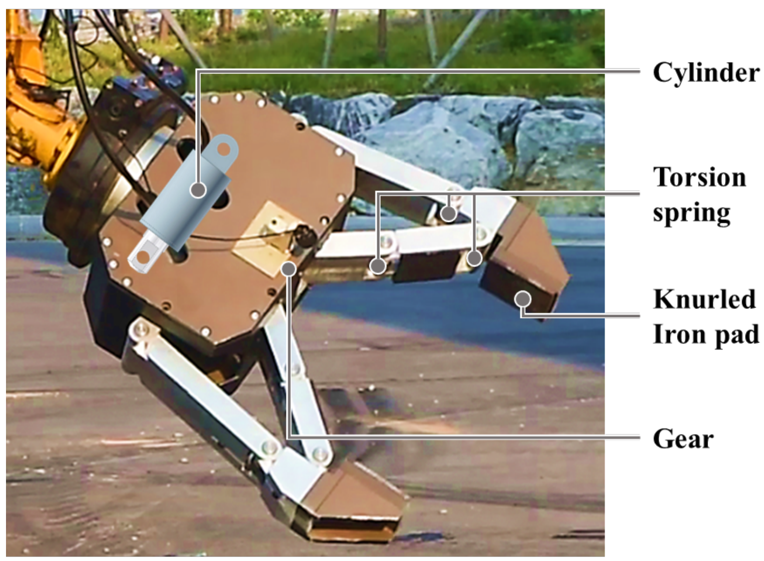

(b)

Figure 5: Configuration of attachments; (a) The multifunctional attachment of the right manipulator, (b) the gripper-type attachment of the left manipulator.

The right side is designed as a multifunctional attachment by tying together the tools needed for precise work. The mechanical structure of the multifunctional attachment is illustrated in Fig. 5(a). Not only need to cutting and crushing but also need for spreading the sandwich panel or open the debris. In addition, it was designed with the structure to increase the rotation function of steel bar or pipe with a diameter less than 40mm. The cylinder was selected based on a cutting force of 350kgf for cutting ϕ20mm rebar. Accordingly, it was designed to have a crushing force of about 220kgf and a grip force of 120kgf, and the blade of the cutter was designed to be 150mm. It is necessary to adjust the gripping force in order to grip various objects of different materials with the pinching part. In this study, a method of controlling the cylinder pressure and controlling the required grip force was adopted. The multifunctional attachment has only 1 DOF and just two simple stages for gripper actuation, closing, and opening. In the current design, a linear actuator is used to actuate the attachment.

Grabs used in construction machinery have different gripping performances depending on the shape of the object. The reason for producing a dedicated grab is to improve the gripping performance and increase the efficiency of work. The finger-type attachment was designed to allow the gripping of objects of various shapes, even if only the pressure of the cylinder is controlled for unstructured objects. The linear actuator is located at the attachment base to actuate the finger-type attachment. The finger joints consist of a four-bar linkage and springs in a complex structure that can adapt to the shape of an object. As it can be seen in Fig.5(b) of the gripper, the finger is connected with a shaft and link mechanism to the actuation. It is possible to control the grasping force by controlling the pressure, and the spring allows for human-like grasping. The required specifications were designed with a gas tank (ϕ 367mm), C-shaped steel (250mm), brick (50mm x 200mm), and cement block (250mm), with concrete debris of less than 400mm, and the weight of a graspable object was selected as 200 kg.

3.2 Driving System

Disaster-responding systems must have a different mechanism from conventional excavators to overcome obstacles and quickly access the disaster site. The most commonly used driving system is the wheel-type, such as a car. Because wheels can move quickly and with relatively high efficiency on flat ground or roads, excavators usually work in downtown areas or around streets. However, the wheel's movement performance on the uneven terrain and the fragile environment is rapidly deteriorating (Visser & Stampfer, 2015). A crawler type is used to solve this problem when designing a driving system for driving in rough terrains. Although the driving speed is slower than that of the wheel-type, it has a wide ground contact area, making it easy to move in rough terrains.

The manipulator is infused with a mobility significance in the crawler-type excavator being able to move on various terrains. Even with a slight obstacle besides the crawler, it is difficult to change direction, requiring much power, and the track may come off or be damaged. Accordingly, the excavator uses the arm to hold the body and switches direction to rotate using one crawler and swing joint. As such, the crawler-type is difficult to change direction in the uneven terrain, and even when overcoming the stepped landscape, it is not easy to move without arms. If the driving system is designed with only the crawler-type, it may take a very long time to access the disaster site or may not be able to overcome it.

The excavator of Menzi Muck, Switzerland, is equipped with four legs and independently driven four wheels (Jelavic, Berdou, Jud, Kerscher, & Hutter, 2020). By controlling the four legs, the posture of the cabin can be maintained horizontally, even in places with terribly slopes or steps. On the sloping terrain, not only wheels are used, but also outriggers are used to move. The excavator of KAISER, Liechtenstein, has presented a model with four crawlers attached and a model consisting of legs and wheels in the same type as Menzi Muck (KAISER, n.d.). By combining the legs and wheels into a hybrid system, increased flexibility comes with an increase in complexity. As the whole-body configurations and the contact schedule of the legs are combined with the rolling constraints of the wheels, the amount of computation for movement is increased. The ETH, Swiss, is researching to maintain a posture to reduce the burden on drivers automatically.

We designed the driving system of the disaster-responding special-purpose machinery by analyzing the existing vehicles based on the disaster response scenarios in the collapse situation conditions. We configured independently driven crawlers while maintaining grip in the uneven terrain at the disaster site, as shown in Fig. 6(a). Obstacles with a height of 50 cm can be climbed only by the crawler itself without the help of other mechanisms, and a four-legged mechanism is applied to overcome rough obstacles that can cross the obstacle by lifting the crawler individually. A mechanism for maintaining the system's posture must be present to enable roll, pitch, and yaw controls while keeping the workers safe and preventing the machinery from overturning while working on a slope. Therefore, to account for the roughness of the ground and the design requirements, the mechanism of the four legs was designed such that each leg could be moved up, down, left, and right through two cylinders (Shin, Ko, Seo, & Hong, 2016). The leg-crawler can raise the system 1.2 m above the ground by controlling the J_{L_1} cylinders and crawlers. The driving system can also maintain the posture of the mainframe according to the ground condition. Since the leg can widen the horizontal distance of the crawlers by controlling the J_{L_2} cylinders of each leg, the system can be driven in a considerably stable posture while working or moving on unstable terrains without installing a separate outrigger. Consequently, the driving system can control the postures up to an angle of $30°$ along the roll axis and up to $25°$ along the pitch axis.

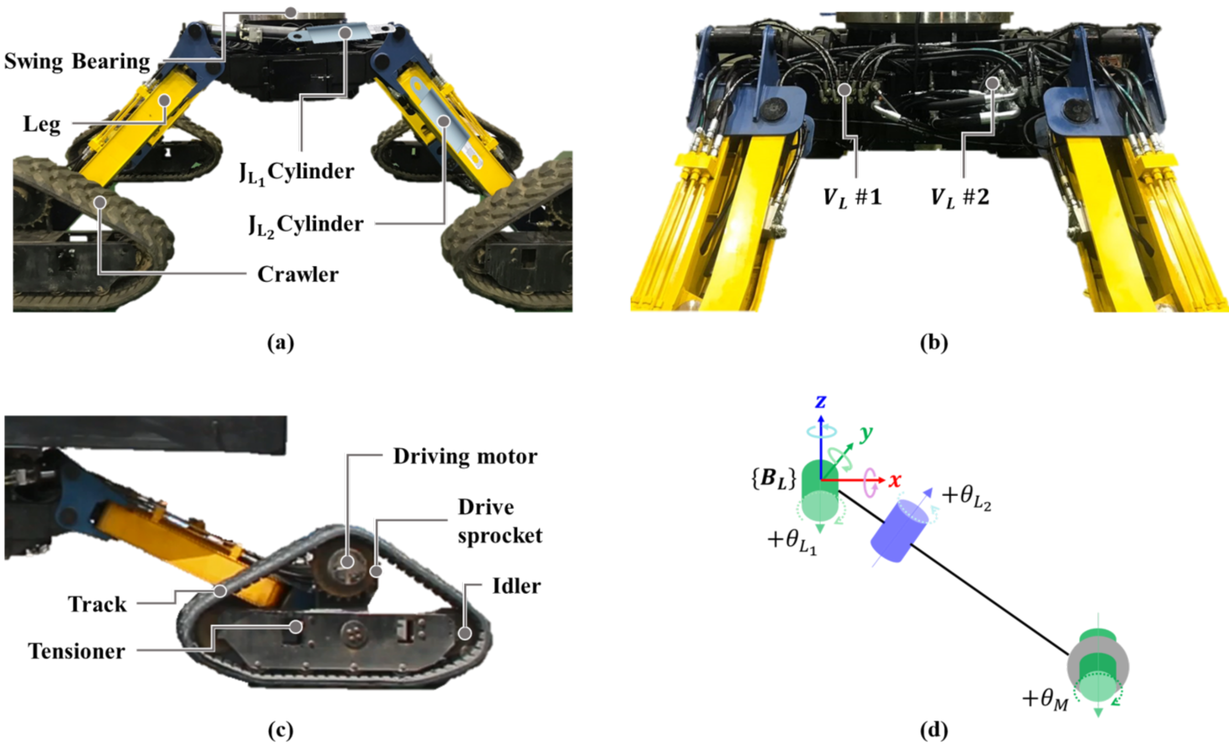

Figure 6: Driving system. (a) The structure of the driving system. (b) The position of the valves. (c) The structure of the crawler. (d) Kinematic layout.

The driving motor was selected to achieve a maximum driving speed of 4.1km/h. The Danfoss PVG 32 valves (V_L #1) were used to control the valves of J_{L_1} and J_{L_2} of each leg and the Danfoss PVG 100 valves (V_L #2) were used to control the driving motor. The control valves were placed on the front and back of the chassis of the driving system, as shown in Fig. 6(b).

The crawler structure consists of a track, driving motor, drive sprocket, idler, and tensioner, as shown in Fig.

6(c). We defined the position of the pinpoint connected to the leg through dynamic analysis. The crawler mechanism was designed to provide posture stabilization. Torsion spring and stopper were designed at the connection point to prevent rotation of the crawler connected to the end of the leg.

Figure 6(d) illustrates the kinematic scheme and joint positioning of the leg-crawler. $\{B_L\}$ is the reference coordinate of each leg-crawler. Joint axes are marked with colored lines. Green and blue represent pitch and yaw axes, respectively. θ_{L_i} is each joint angle of the leg-crawler. θ_{L_m} is the driving motor angle.

3.3 Cabin

The special-purpose machinery is typically controlled by a person present in the cabin. Thus, it must be designed according to the driver's workspace, the field of view, and convenience. In addition, it is vital to consider the combination of the hydraulic line, which delivers hydraulic fluid from the power pack, with the mainframe to operate the dual-arm manipulators and the driving system.

The cabin was designed according to the work area of the controller used by the driver to control the entire system from its center, as shown in Fig. 7. The engine control panel may check the state of the power pack, start the engine, adjust the rpm, and adjust the pressure of each pump. The left/right arm master device was designed to consider the range of human motion and mechanisms for less fatigue. The master system for operating the driving system is configured to be controlled only with both feet of the operator. It consists of pedal A, which controls the driving speed, and pedal B, which can give up/down height adjustment commands.

The outer frame of the machinery was designed with bent pipes and wire meshes. The size of the cabin, which was designed according to the workspace of the controller and the sizes of the mainframe and power pack, was equal to 1.78 m x 1.44 m x 1.5 m. The right side of the cabin was designed for placing the controller components, and the left side was designed to accommodate the uninterruptible power source (UPS) to supply power to the controller. The door was placed on the left side due to the positions of the dual-arm manipulators and the controller. The front portion of the cabin was designed according to the viewing angle of the driver while working with both arms. Polycarbonate was applied to the chassis to protect it from external materials and noise. At the bottom of the cabin, sufficient space was retained for the swing motor and the hydraulic hoses connected to the dual-arm manipulators and the driving system. In addition, a fastening component was designed according to the cabin mounting method.

(a)

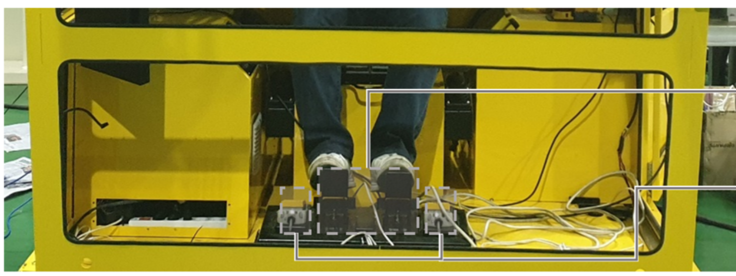

(b)

Figure 7: Cabin system. (a) The configuration of the cabin system. (b) Pedal configuration to control the driving system.

3.4 Hydraulic System

The specifications of the power pack were defined according to the requirements of a machine weighing 5 tons. The engine and pump models were selected according to the results of the hydraulic simulation, the performance of functioning machinery, and future commercialization requirements (Lee, Noh, Jang, & others, 2018)(Choi, Le, & Yang, 2019). The Doosan D24 engine was chosen for the proposed machinery. It is a 4-cylinder turbo-diesel engine with a power output of 55kW (75HP) and satisfies the Tier 4 Final emission regulations. This ensures that the system would be commercially viable in the future. Two remote pressure-compensated axial piston pumps, which are part of Danfoss' Series 45 pumps, were connected to the system. Pump 1 was used to drive the dual-arm manipulators and the drive motor, while Pump 2 was used to drive the legs of the driving system. Pump 1 has a maximum pressure and flow rate of 230 bar and 71 cm^3/rev, respectively, and Pump 2 has a maximum pressure and flow rate of 250 bar and 25 cm^3/rev, respectively. The power pack includes the engine, engine control panel, battery, cooling system, hydraulic pumps 1 and 2, housing and coupling for establishing connections, and hydraulic parts for generating and supplying hydraulic pressure, as shown in Fig. 8. It also has brackets to fix the fuel tank, hydraulic oil tank, and hydraulic block valve. The volume of the hydraulic oil tank was chosen to be 140L on the basis of the predicted flow rates of the special-purpose machinery. In addition, a radiator and a cooling fan were installed to cool the hydraulic oil.

Unlike construction machinery, which focuses on work efficiency, disaster equipment requires its hydraulic system control to vary the force required, depending on the nature of the work. The pump pressure is set according to the force required for the task, and the engine's rated speed is set according to the maximum work speed of the task. The dual-arm manipulator uses a proportional electronic pressure compensation control method that allows the rider to set the pump pressure and maintain it according to the characteristics of the task and its corresponding force requirements. In addition, a flow control method linked to the engine load was adopted to minimize the engine stops and engine speed fluctuations due to variations in the instantaneous workload.

The load sensing method was adopted to control the leg posture and the driving motor of the driving system. Load sensing control is a method of supplying the minimum required flow rate and pressure to the actuators and the motor while mechanically controlling the pump discharge to achieve a constant pressure difference across the flow control valve next to the pump. Thus, these designs allow special-purpose machinery to appropriately distribute the hydraulic pressure according to the load while working and moving on uneven terrain. This allows the machinery to deliver an optimal performance at disaster sites.

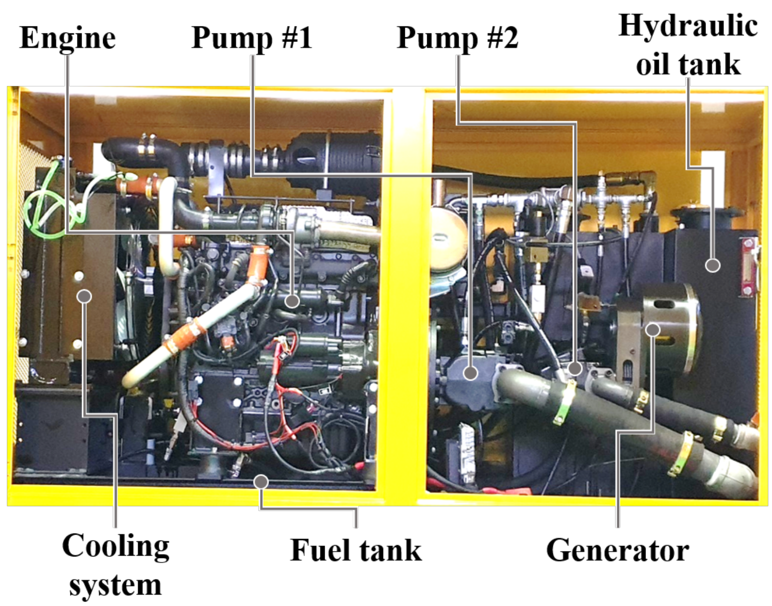

Figure 8: Configuration of the power pack.

3.5 System Integration Design

System integration refers to the integration of a series of processes, including the development, construction, and operation of systems. We designed the overall layout of the system to optimize the operations according to the design objective of each component. The system was further optimized for weight distribution to prevent it from overturning. This was carried out by accounting for the total weight, testing the functions of each component, and conducting simulations to ensure the workability of the overall system in different scenarios. Through this process, the binding positions of the mainframe, dual-arm manipulators, driving system, cabin, and power pack were determined.

The mainframe, which is where all the modules are combined, was designed by performing a stiffness analysis simulation to obtain the stiffness that would be sufficient to carry out the specified operations. It was fabricated as a welded structure. The mainframe was connected to the driving system through a swing bearing and a center joint to enable free rotation, as shown in Fig. 9(a). The center joint was designed to supply the hydraulic pressure required for controlling the leg and rotating the crawler of the driving system. This hydraulic pressure was generated by the power pack. The swing bearing was connected between the mainframe and the driving system. It had sufficient durability in dynamic conditions and also accounted for the maximum load condition of the manipulators and the weight of the system. The design of the cabin mount device accounted for the interference caused between the swing motor, power pack, and cabin mounting method. The components were arranged according to the center of gravity and the overall height of the system. The rotation of the hydraulic hose, power line, and communication line was prevented by mounting the center joint and slip ring, as shown in Fig. 9(b).

The engine power pack system was installed in the mainframe. It consisted of hydraulic components to drive the machinery. The spaces in the mainframe were designed to place and mount components like the engine, pump, cooling device, hydraulic oil tank, and fuel tank. The system exterior comprises a cover chassis to protect various components from external shock.

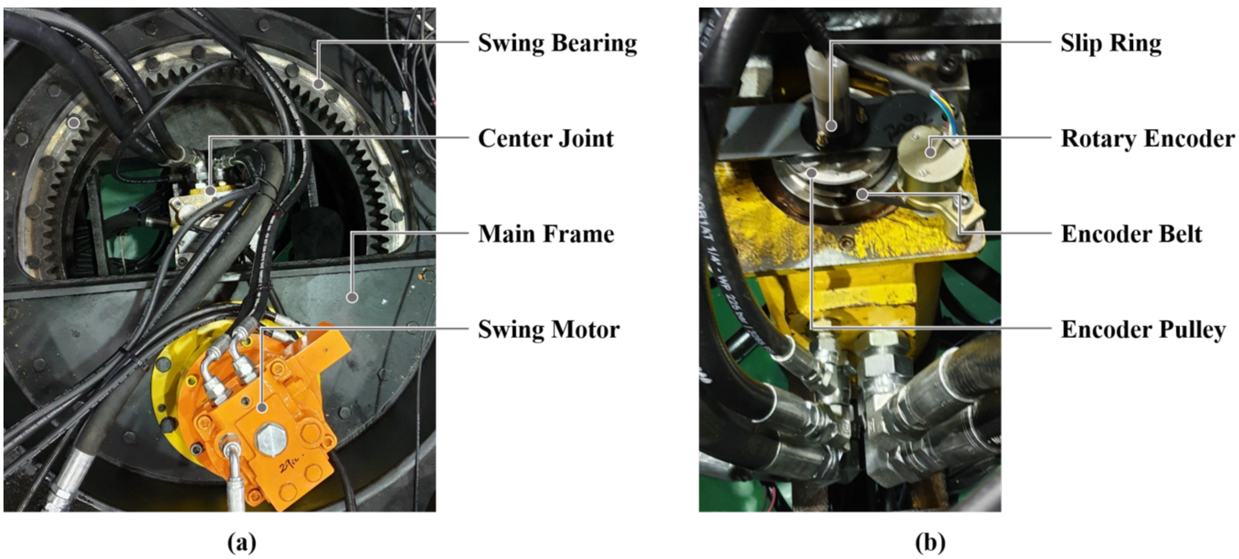

Figure 9: The structure for the integration of dual-arm manipulator and the driving system. (a) The swing joint. (b) The center joint.

4. CONTROL ARCHITECTURE

4.1 Algorithm

The special-purpose machinery proposed in the current study comprises 14 DOF dual-arm manipulators, swing joints, attachments, four legs, and crawlers. This machinery requires a system to provide the driver with sufficient control to perform complicated tasks by manipulating the machinery. Different manipulation and control methods adopted by existing excavators that move one joint with one lever are needed to control the dual-arm manipulators simultaneously. The control system used to control the movements of the left and right manipulators with the left and right controllers was designed by combining the driver's movements with robotic control technology. In robotics, human control of the robot arm is referred to as the master-slave control. The control algorithm from our previous study was configured to enable the dual-arm manipulators to perform tasks by moving according to the movement of the two arms of the driver holding the master device, as shown in Fig. 10. The Marionette algorithm for intuitive control of 'as if the operator's arm is moving' was presented as a control strategy for dual-arm manipulators with attachment. In Fig. 10, $\vec{P}_{T_m}$ is the position and orientation sensed by the master device. $\vec{P}_{T_s}$ is the current position and orientation of the slave robot's end-effector. $\vec{F}_m$ is the force generated by the master haptic device. $\vec{u}_s$ is the control laws to be designed in the slave controllers (Kim, Park, Han, Kim, & Cho, 2020). When the load of the slave robot becomes heavier, the feedback force increased with the load.

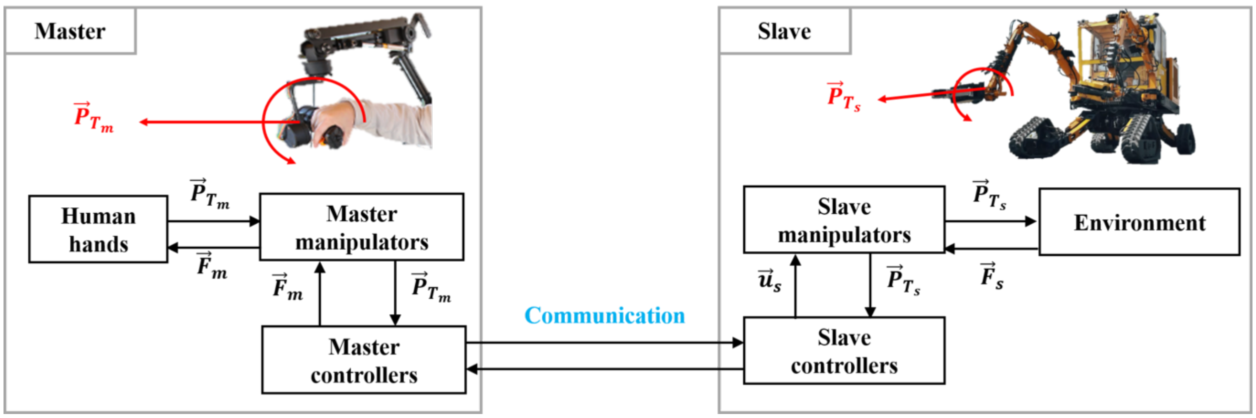

Figure 10: Block diagram of control strategy of the dual-arm Manipulator.

We developed a master device. The joystick can be held by a human hand and pushed in the desired direction on the reference coordinate $\{m\}$ to generate an input along the x, y, and z axes. The ROM of this controller was designed according to the range of convenient movement of both arms of the driver in the cabin. Since the wrist of the controller has 3 DOFs, it is possible to generate inputs in the roll, pitch, and yaw directions on the reference coordinate $\{m\}$. Thus, the operator can generate inputs in certain directions by moving the controller to the desired position. There are buttons on the joystick. The operator can grip the joystick and control the master device while pressing the buttons with the operator's thumb. We assigned the joystick button to operate a closing/expansion of the attachments and the swing joint's clockwise/counterclockwise angle input.

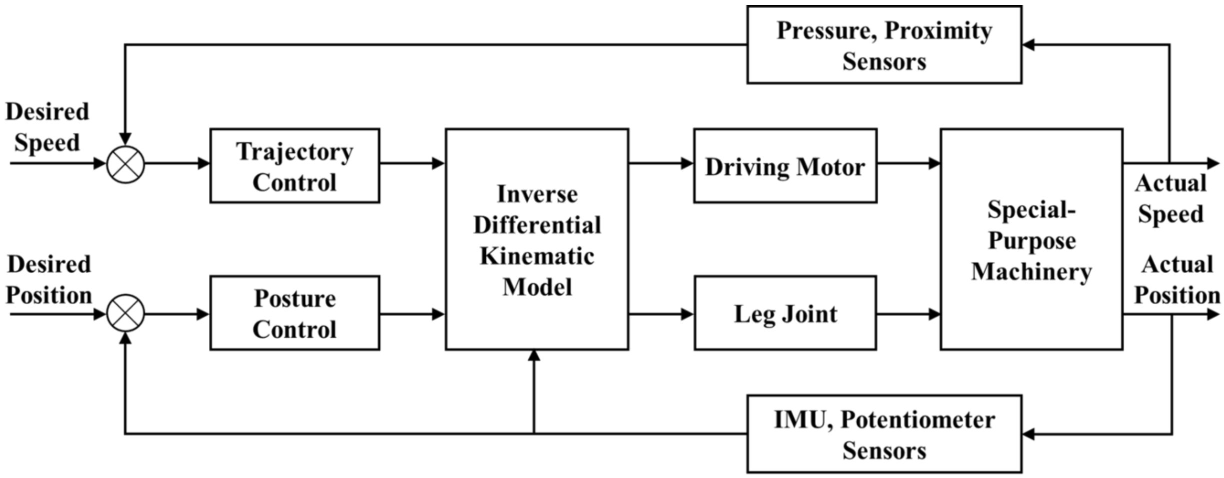

Figure 11: Block diagram of control strategy of the driving system.

The driving system comprises four 2 DOF legs, with an independently driven crawler attached to the end of each leg. The disaster-responding special-purpose machinery cannot carry out an initial rapid response by controlling each leg or using the manipulators to move on an uneven surface in a disaster situation. A simpler method for moving while performing tasks is required because both arms of the operator are holding the controllers of the manipulators. Therefore, we have added four pedals to control the driving system. The driving pedal A can move back and forth from its initial position. The left and right driving pedals A generated forward and reverse inputs for the two left and two right crawlers, respectively. This allows the implementation of forward/reverse and turn operations. In addition, there is a need for a method of generating an input to adjust the machine's height. The up/down pedals B were allocated to generate an upward (right) and downward (left) input, respectively. The system was designed to control the height by simultaneously moving the legs and the crawlers. In addition, the system was designed to move while maintaining the posture of the mainframe on a slope without separate leg control through a hydraulic system composition that includes a load sensing pump and an algorithm to control the leg joints according to the load of each leg, as shown in Fig. 11.

The hydraulic system of the independently driven crawlers consists of a swash plate-type load sensing pump (Pump #2), the electronic proportional main control valves with pressure compensated flow control function (V_L #2), and driving motors. As the electronic proportional control signal increases, the spool of the main control valve is gradually switched, and the pump flow rate way into the driving motor. And then, the load pressure sensed by the pressure sensor mounted on the driving motor is feedback to the pressure compensation valve so that the constant flow rate flows in proportion to the spool opening. The load-sensing pressure is transferred to the pump regulator, and the pump discharge flow rate is determined by the difference between Pump #2 and the driving motor pressure. Accordingly, even if the driving load condition is applied differently to the 4-crawlers, the uniform flow rate distribution is achieved so that it is possible to secure the synchronization of the driving motors and the straightness of the driving (Lee, Kim, Lee, Kim, & Kwon, 2017).

The mathematical model for posture control of the driving system was composed of a differential kinematic model-based control algorithm (Ha et al., 2016). A mathematical model of a single crawler-leg system is generated, and the mathematical model for the entire driving system is obtained from the single mathematical model. As desired input to the control algorithm, the posture control algorithm is configured with desired roll and pitch angles. A height of the mainframe is given a driving speed and a height of the mainframe from the ground through the IMU sensor and contact condition. As desired input to the control algorithm, the desired roll and pitch angles as constant values is 0 degrees, and the driving speed and the height of the mainframe from the ground can be given through the pedal devices in the cabin. Contact conditions can be estimated through IMU mounted on the mainframe, pressure sensors and potentiometers mounted on the legs, and driving motor speed sensors.

4.2 Control Network System

As a control system for the special-purpose machinery, it has been developed based on optimized embedded systems for distributed interfaces of local devices (actuators and sensors) and high-performance PC systems for centrally collecting and processing data from local devices. We are shown in Fig. 12 to represent the structure of the entire control loop and the control loop of each module in a block diagram.

This control network system is configured based on a general real-time operating system (Ubuntu+Xenomai), considering each system's fast and accurate data exchange and operation characteristics. It is a system that can guarantee a control cycle of up to 2 kHz with various communication network combinations such as EtherCAT, RS485, and Socket (TCP, UDP).

We applied EtherCAT communication for the real-time exchange of massive data (Control Inputs of valves, sensors) between the PC system responsible for control calculation and local devices of the dual-arm manipulator and the driving system. RS485 communication, which enables high-speed multi-communication with minimal resources (cost, size, development level), is applied between the JCU (Joint Control Unit) systems that perform low-level joint control. Socket communication, which has characteristics that remote access to devices, is used to data exchange with the master devices for the driving system and the dual-arm manipulator in the cabin.

The JCU system for joint control and the Bridge relay system using DPRAM (Dual-Ported RAM) for cross-communication data sharing are custom-made embedded systems based on ARM Coretex-M4. We combined local devices in consideration of each module position and operation. It was configured by minimizing exposure to the platform.

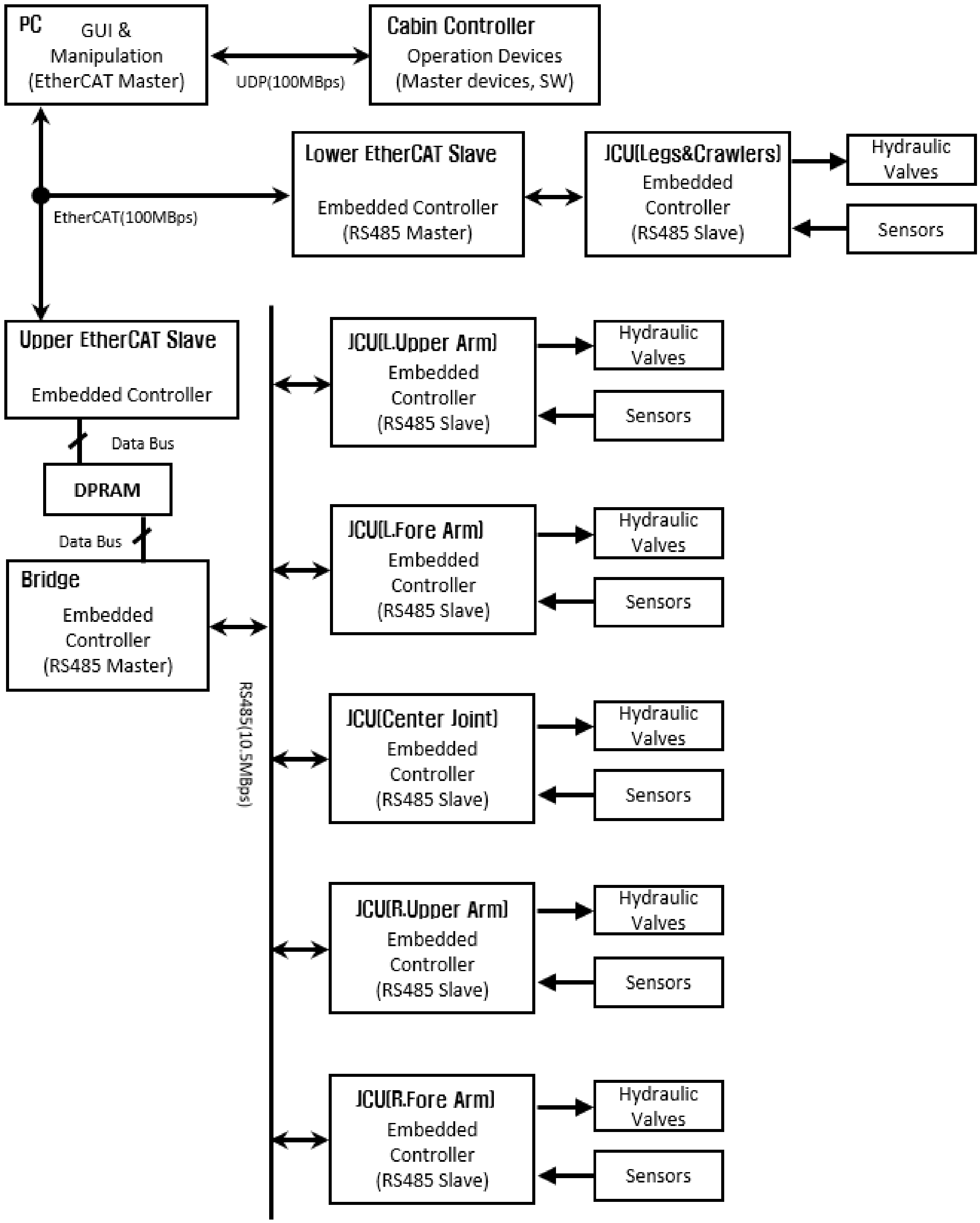

Figure 12: Structure of the Control Network System.

5. EXPERIMENTS

This chapter describes the tests performed at the test site to evaluate the performance of the special purpose machinery in disaster scenarios. In order to create lifesaving work scenarios and representative work modes at building collapse sites and use them to evaluate system performance, we developed a test site, based on a simulated disaster environment, for performance evaluation, as shown in Fig. 13. We have simulated events that may occur in lifesaving rescue tasks at disaster sites as a series of processes and defined tasks by using the work modes according to the target specifications of the special purpose machinery. In a situation wherein a person is trapped under collapse debris and needs to be rescued from a building collapse site, the machinery overcomes the rough environment and reaches the target point through the driving scenario. The buried person is then rescued by using the machinery to safely removing the collapse debris through the work scenario. The work target specifications of each mode are outlined in Table 1.

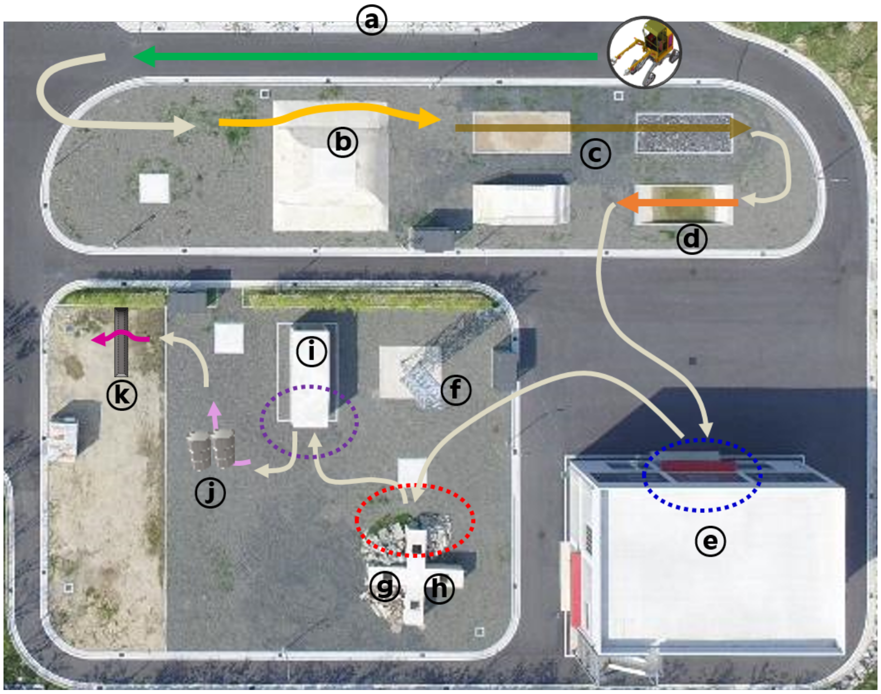

Figure 13: Scenario test site: (a) Flat surface, (b) Lateral slope, (c) Uneven surface, (d) Longitudinal slope, (e) Lifting pipe, (f) Lifting tire, (g) Crushing brick, (h) Cutting rebar, (i) Tearing of sandwich panels, (j) Pushing drum barrel, (k) Overcoming obstacle.

The results of flat ground driving, among driving scenarios, are shown in Fig. 14(a). The operator drove on the machinery on a 60m flat ground made of asphalt by using the forward/reverse pedal A in the cabin. The speed was measured by using a prism that was mounted on the cabin. The prism reflects a laser beam, which measures the change in position. The driving speed was found to be 4.1km/h.

Figure 14(b) shows the result of driving on a slope. The machinery maintained the horizontal orientation of the mainframe while driving with the left and right crawlers at low and high points on a 15° lateral slope. In addition, the mainframe was kept horizontal when the crawlers entered the 11° vertical slope, as shown in Fig. 14(c). At this time, the operator only controlled forward/reverse pedal A. This result reveals that the algorithm for adjusting the leg joints according to the loads on the hydraulic system, including the load-sensing pump and every other pump, is working.

For rough ground driving, a task of driving through a ground consisting of debris, which is 10cm or smaller, was performed, as shown in Fig. 14(d). At this time, the operator only controlled forward/reverse pedal A, and the stable driving characteristic of the machinery was verified.

The difficulty of the task was increased by including steel frame obstacles with a height of 50cm and a slope angle of 37°, as shown in Fig. 14(e). The machinery also passed over the installed obstacles safely.

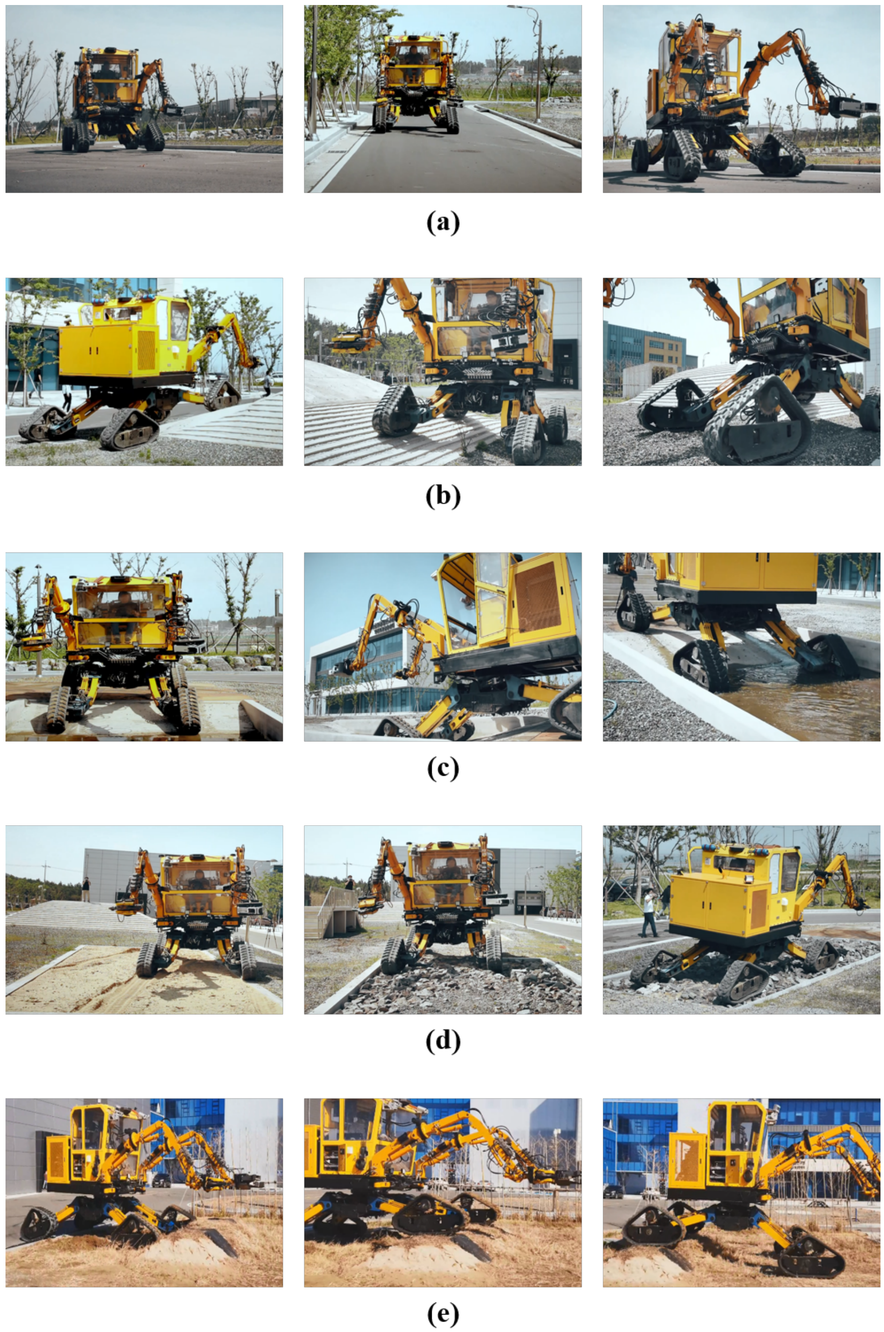

Figure 14: Driving test results. (a) Flat surface, (b) Lateral slope, (c) Longitudinal slope, (d) Uneven surface, (e) Overcoming obstacle. Link

A test was performed for a situation where a person is lying under a pipe in a factory and the special-purpose machinery enters the factory and supports the rescue task, as shown in Fig. 15(a). First, to pass through the factory gate and enter the factory, the height of the machinery was lowered by controlling pedal B. Then, the operator approached the buried person by controlling pedal A and removed the pipe from the buried person, as shown in Fig. 15(b).

A snapshot of the lifting process is shown in Fig. 15(c). The task of picking up a 200kg tire on the driving path, rotating and moving it with a swing joint was performed. In addition, a test was conducted to verify whether the design specification for lifting 1 per arm and lifting 200kg. The position and orientation of the attachment were adjusted to grasp the inner surface of the tire. After lifting the tire, the swing joint was moved to remove the tire in the driving path.

The result of performing the crushing work mode is shown in Fig. 15(d). The manipulator was operated to position the brick between the crushers of the multifunctional attachment, and then the brick was crushed by the attachment. The results of the cutting task are shown in Fig. 15(e). The operator controlled the left manipulator to grasp the rebar and simultaneously controlled both arms to position the rebar at the location of the shear of the multifunctional attachment of the right manipulator. And it was confirmed that the rebar was cut by manipulating the multifunctional attachment. It can be observed that the seven joints move simultaneously to move the endpoint of the manipulator to the target point, instead of moving each joint separately by the operator. This confirms that the endpoint position of the 7 DOF manipulator can be controlled intuitively using the proposed controller of the dual-arm manipulators and that concrete blocks can be crushed using the attachment. It also confirmed that it can grasp and move an object and simultaneously perform other tasks such as cutting another manipulator through the operating method.

The results of the spreading task are shown in Fig. 15(f). It can be observed that space is secured by drilling and breaking through a wall blocked by 0.5 mm thick corrugated iron using the multifunctional attachment to secure access and rescue passage for firefighters.

The results of the pushing task are shown in Fig. 15(g). This task involves pushing a drum on the ground to a distance by simultaneously controlling the swing joint and dual-arm manipulator. This shows that the endpoint of the manipulators and the swing joint can be easily controlled simultaneously.

Figure 15: Working test result. (a) Enter the factory, (b) Lifting pipes, (c) Lifting tire, (d) Crushing brick, (e) Cutting rebar, (f) Tearing of sandwich panels, (g) Pushing drum barrel. Link

We performed experiments in addition to the proposed scenario to confirm the performance of dual-arm cooperation. In the case of objects that are difficult to grasp with one arm, both arms can be moved to work as shown in Fig. 16(a). It is a task to operate both arms simultaneously to position both ends of the drum barrel and lift both arms by applying force in the direction toward the object. This test verified the lifting power of the fabricated dual-arm manipulators, and it can be observed that the developed operating method allows the operator to manipulate the swing joint while performing a task by controlling dual-arm manipulators through the smart controller.

The results of the pouring water into the water bottle are shown in Fig. 16(b). First, the dual-arm manipulator picked up each of the empty barrels and containing water on the floor. It can be confirmed that the positions and angles of the dual-arm manipulator are simultaneously changed to pour water.

The results of the lifting long pipes are shown in Fig. 16(c). To lift the long pipe, the dual-arm manipulator must hold both ends and lift it. First, you can see that you lift it slightly with the right arm, then grab it with the left arm and lift it. Through this, it can be confirmed that the dual-arm manipulator can perform each task simultaneously.

Figure 16: The dual-arm cooperation test. (a) Lifting drum barrel, (b) Pouring water into the water bottle, (c) Lifting long pipes. Link

The above test results verified that one operator can ride and control the special-purpose machinery. Furthermore, the performance of the developed special-purpose machinery was evaluated by performing predefined tasks in a disaster environment.

6. CONCLUSION

This study describes the design and fabrication of special-purpose machinery for lifesaving and recovery support for a rapid initial response within the golden hour after the occurrence of disasters. We derived the design parameters by defining tasks through the analysis of scenarios in disaster-responding situations and existing special-purpose machinery. Based on the results of this analysis, the special-purpose machinery was fabricated, and its components were described in detail, including dual-arm manipulators, leg-crawlers, mainframe, cabin, power pack, and control networks. In addition, we introduced a system for operators to intuitively operate a system comprising dual-arm manipulators and four legs with crawlers attached to the end of the legs.

The tests performed at a test site for evaluating performance based on disaster scenarios conducted to verify the work performance of the integrated special-purpose machinery were described. The tasks were largely classified into the driving mode and work mode. The results confirmed that the rough environment could be overcome and the target point reached through the driving mode, and the collapse debris was safely removed through the work mode. These tests verified that one operator can ride and control the developed special-purpose machinery, and the performance of the developed special-purpose machinery was demonstrated through the defined tasks.

Acknowledgment

This work was supported by the Technology Innovation Program(10052968, Development of core components and systems for special purposed machine in disaster environment) funded By the Ministry of Trade, Industry & Energy(MOTIE, Korea) and in part by the Korea Institute of Industrial Technology as “Development of industrial robot and post-processing robot application technology for Ppuri industry (KITECH JH210015)” project.

References

Bagheri, M., Ajoudani, A., Lee, J., Caldwell, D. G., & Tsagarakis, N. G. (2015). Kinematic analysis and design considerations for optimal base frame arrangement of humanoid shoulders. *2015 IEEE International Conference on Robotics and Automation (ICRA)*, 2710–2715. IEEE.

Brantner, G., & Khatib, O. (2020). Controlling Ocean One: Human–robot collaboration for deep-sea manipulation. *Journal of Field Robotics*, *38*(1), 28–51. https://doi.org/10.1002/rob.21960

Cho, J.-S., Park, S.-S., Kim, J.-T., Park, B.-Y., Bae, J.-H., Lee, D.-H., … Park, S.-D. (2016). Design of Dual Arm Manipulator for a Disaster-Responding Special Purpose Machinery. *Journal of Drive and Control*, *13*(4), 95–101.

Cho, J. S. (2018). Design of Attachments for Dual Arm of Disaster-Responding Special Function Machinery by TRIZ. *Journal of Drive and Control*, *15*(3), 29–35.

Choi, S. W., Le, Q. H., & Yang, S. Y. (2019). A Study on Hydraulic Simulation Analysis of a 7 DOF Dual Arm Machinery. *2019 23rd International Conference on Mechatronics Technology (ICMT)*, 1–4. IEEE.

Delmerico, J., Mintchev, S., Giusti, A., Gromov, B., Melo, K., Horvat, T., … Scaramuzza, D. (2019). The current state and future outlook of rescue robotics. *Journal of Field Robotics*, *36*(7), 1171–1191. https://doi.org/10.1002/rob.21887

Ha, J. W., Kim, S. H., Lee, Y. S., Sun, D. I., Jang, S. H., & Han, C. S. (2016). A Study on the Modeling of Independently Driven Quadruped Crawler System for Posture Control of Special Purpose Machine for Disaster Response. *Journal of Drive and Control*, *13*(4), 82–88.

Ishii, A. (2006). Operation system of a double-front work machine for simultaneous operation. *Proc. Int. Symp. Automation and Robotics in Construction*, 539–542.

Ito, M., Raima, C., Saiki, S., Yamazaki, Y., & Kurita, Y. (2021). Effects of Machine Instability Feedback on Safety During Digging Operation in Teleoperated Excavators. *IEEE Access*, *9*, 28987–28998. https://doi.org/10.1109/access.2021.3059710

Jelavic, E., Berdou, Y., Jud, D., Kerscher, S., & Hutter, M. (2020). Terrain-Adaptive Planning and Control of Complex Motions for Walking Excavators. *2020 IEEE/RSJ International Conference on Intelligent Robots and Systems (IROS)*. https://doi.org/10.1109/iros45743.2020.9341655

Jeong, D., Kim, C., Kim, J. H., Suh, J., & Jin, M. (2017). Mission Scenario-based Design of Hydraulic Manipulators for Armored Robot Systems. *Journal of Drive and Control*, *14*(4), 51–60.

KAISER. *Mobile Walking Excavator*. Retrieved from https://www.kaiser.li/products/s2-emission-stage-eu-iiia/

Kim, J. T., Chon, S., Park, S., Kim, J., Lee, S., & Cho, J. (2020). Experimental Investigation of a Disaster-Responding Special Purpose Machinery. *Conf. of The Korea Fluid Power Systems Society*, 107–108.

Kim, J. T., Park, S., Han, S., Kim, J., & Cho, J. (2020). Control Strategy and Verification of Dual-Arm Manipulator for Disaster-Responding Special Purpose Machinery. *Journal of Drive and Control*, *17*(4), 31–37.

Klamt, T., Schwarz, M., Lenz, C., Baccelliere, L., Buongiorno, D., Cichon, T., … Behnke, S. (2019). Remote mobile manipulation with the centauro robot: Full-body telepresence and autonomous operator assistance. *Journal of Field Robotics*, *37*(5), 889–919. https://doi.org/10.1002/rob.21895

Lee, G. H., Noh, D. K., Jang, J. S., & others. (2018). Design feasibility study by analytical approach for a disaster response hydraulic driving system. *Journal of Drive and Control*, *15*(2), 22–31.

Lee, H. J., & Brell-Cokcan, S. (2021). Cartesian coordinate control for teleoperated construction machines. *Construction Robotics*, *5*(1), 1–11. https://doi.org/10.1007/s41693-021-00055-y

Lee, S. H., Kim, D. M., Lee, Y. S., Kim, S. H., & Kwon, S. D. (2017). The Characteristic Analysis of Travel Hydraulic System of 4 Wheel Drive with Pressure Compensated Function for a Special Purpose Machinery. *Conf. of The Korea Fluid Power Systems Societyue here*, 78–83.

Machinery, H. C. (2012). *Double Arm Working Machine*. Retrieved from https://www.hitachicm.com/global/businesses/products/double-arm-working-machine/

Mascaro, R., Wermelinger, M., Hutter, M., & Chli, M. (2020). Towards automating construction tasks: Large-scale object mapping segmentation, and manipulation. *Journal of Field Robotics*, *38*(5), 684–699. https://doi.org/10.1002/rob.22007

Montazeri, A., & Ekotuyo, J. (2016). Development of dynamic model of a 7DOF hydraulically actuated tele-operated robot for decommissioning applications. *2016 American Control Conference (ACC)*, 1209–1214. IEEE.

Nishida, T., Koga, H., Fuchikawa, Y., Kitayama, Y., Kurogi, S., & Arimura, Y. (2006). Development of pilot assistance system with stereo vision for robot manipulation. *2006 SICE-ICASE International Joint Conference*, 2675–2680. IEEE.

Park, S. H., Jin, M., Kim, Y.-R., Kim, D., Kim, J.-S., Shin, D. B., & Suh, J. (2018). Vehicle body design of armored robot for complex disaster. *The Journal of Korea Robotics Society*, *13*(4), 248–255.

Robotops, T. (2009). *Walking robot crane.* Retrieved from https://www.youtube.com/watch?v=YD4w2e69VUk

S, M. C., Sairam, P. S., Veeramalla, V., Kumar, A., & Gupta, M. K. (2020). Design and Analysis of New Haptic Joysticks for Enhancing Operational Skills in Excavator Control. *Journal of Mechanical Design*, *142*(12). https://doi.org/10.1115/1.4048462

Shin, D. B., Ko, Y. H., Seo, W. S., & Hong, D. H. (2016). Design of a robot leg mechanism for early rescue and recovery support from a disaster. *Journal of Drive and Control*, *13*(4), 89–94.

Visser, R., & Stampfer, K. (2015). Expanding Ground-based Harvesting onto Steep Terrain: A Review. *Croatian Journal of Forest Engineering: Journal for Theory and Application of Forestry Engineering*, *36*(2), 321–331. Retrieved from https://hrcak.srce.hr/151831

Sarcos Guardian® GT Robot. (2018). *Force-Multiplying Dexterous Robotic System.* Retrieved from https://www.sarcos.com/products/guardian-gt/